Journal Pre-proof

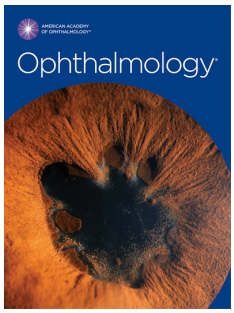

Neuroretinal and RPE changes and susceptibility to Age-Related Macular Degeneration: insights from the longitudinal Alienor Study

Petra P. Larsen, Marie-Noëlle Delyfer, Cédric Schweitzer, Jean-François Korobelnik, Cécile Delcourt

PII: S0161-6420(25)00003-X

DOI: https://doi.org/10.1016/j.ophtha.2025.01.002

Reference: OPHTHA 13027

To appear in: *Ophthalmology*

Received Date: 27 September 2024

Revised Date: 23 December 2024

Accepted Date: 2 January 2025

Please cite this article as: Larsen PP, Delyfer M-N, Schweitzer C, Korobelnik J-F, Delcourt C, Neuroretinal and RPE changes and susceptibility to Age-Related Macular Degeneration: insights from the longitudinal Alienor Study, *Ophthalmology* (2025), doi: https://doi.org/10.1016/j.ophtha.2025.01.002.

Neuroretinal and RPE changes and susceptibility to Age-Related Macular Degeneration: insights from the longitudinal Alienor Study

Petra P. Larsen[1*]; Marie-Noëlle Delyfer[1,2,3]; Cédric Schweitzer[1,2]; Jean-François Korobelnik[1,2]; Cécile Delcourt[1,3]

1 University of Bordeaux, INSERM, BPH, U1219, F-33000 Bordeaux, France
2 CHU de Bordeaux, Service d'Ophtalmologie, F-33000, Bordeaux, France
3 FRCRnet, F-CRIN network, France

Short Title: Macular layer changes and susceptibility to AMD
Keywords (not already present in the title): OCT, clinical (human) or epidemiologic studies: polygenic risk score, genetic risk, imaging

***Correspondence**:
Petra P. Larsen
University of Bordeaux, INSERM, BPH, U1219
146 rue Léo Saignat
33076 Bordeaux Cedex
France
petra.larsen@u-bordeaux.fr

This article contains additional online-only material. The following should appear online-only: Figures S2, S4; Tables S2, S4 – S8.

Abbreviations: AMD: age-related macular degeneration, BLamDs: basal laminar deposits, BM: Bruch's membrane, CFH: complement factor H, CNV: choroidal neovascularization, ETDRS: Early Treatment Diabetes Retinopathy Study, GA: geographic atrophy, GWAS: genome-wide association study, HR: hazard ratio, GCL: ganglion cell layer, INL: inner nuclear layer, IPL: inner plexiform layer, IRL: inner retinal layers, ONL: outer nuclear layer, OPL: outer plexiform layer, ORL: retina retinal layers, PRS: polygenic risk scores, PSL: photoreceptor segment layer, RPE: retinal pigment epithelium, RNFL: retinal nerve fiber layer, SD-OCT: spectral-domain optical coherence tomography, SNP: single nucleotide polymorphism, TRL: total retinal layers.

Financial Support: German Research Foundation grant PL 5077/1-1, Théa Pharma, University of Bordeaux, National Research Agency (ANR 2010-PRSP-011 VISA), Club Francophone des Spécialistes de la Rétine, French Ministry of Health (PHRC, 2012, PHRC12_157 ECLAIR), Fondation Voir et Entendre, Retina France.
Declaration of Interest: P Larsen : none | M Delyfer: Consultant: Abbvie, Bayer, Horus Pharma, Novartis, Roche| J Korobelnik: Consultant: Abbvie, Apellis, Eyepoint Pharma, Bayer, Ocular therapeutix, Ocuphire, Roche, Théa, Carl Zeiss Meditec | C Schweitzer: Consultant: Alcon, Elios, Glaukos, Horus, Bausch+Lomb, Santen, Théa | C Delcourt: Consultant: Allergan, Chauvin-Bausch+Lomb, Théa, Novartis.

Abstract

Purpose: We assessed the associations of macular layer thicknesses, measured using spectral-domain OCT (SD-OCT), with incident age-related macular degeneration (AMD) and AMD polygenic risk scores (PRS).

Design: Population-based cohort study

Participants: 653 participants of the Alienor study, with biennial eye imaging from 2009 to 2024.

Methods: Macular layer thicknesses of eight distinct layers and three compound layers were automatically segmented based on SD-OCT imaging of the macula. Total and pathway specific PRS were calculated from previous AMD genome-wide association studies summary statistics. Associations of macular layer thicknesses with incident intermediate and advanced AMD were analyzed using time-dependent Cox proportional hazards models. Associations of macular layer thicknesses with PRS were assessed using linear mixed models.

Main outcome measures: Incident intermediate and advanced AMD based on fundus colour photographs and SD-OCT.

Results: Mean age at first OCT examination of the 653 participants was 82.2 ± 4.2 years and 61.3 % were women. In multivariate adjusted models, incident intermediate AMD was associated with thicker retinal pigment epithelium (RPE) - Bruch's Membrane (BM) complex in the 1 mm central circle (Hazard ratio (HR)= 1.13 for 1 µm increase; P_{FDR}= 8.08 x 10^{-4}). Incident advanced AMD was associated with thicker RPE-BM complex in both the

central circle (HR= 1.09; P_{FDR}= 0.005) and the inner circle (1 mm – 3 mm) (HR= 1.28; P_{FDR}= 1.61 x 10^{-5}).

Over the study period, RPE-BM complex thickening in the inner circle was more pronounced in individuals with high total PRS (ß= 0.06 µm/year for 1 standard deviation increase, P_{FDR}= 1.61 x 10^{-10}), high complement pathway PRS (ß= 0.04 µm/year, P_{FDR}=3.23 x 10^{-5}), high lipid pathway PRS (ß= 0.03 µm/year, P_{FDR}= 3.74 x 10^{-4}) and ARMS2 (ß= 0.03 µm/year, P_{FDR}= 0.002). Further, high total PRS and high complement-specific PRS were associated with thinner photoreceptor segment layer (PSL) at baseline and with thinning of the outer nuclear layer over the study period.

Conclusion: These results highlight the importance of RPE-BM complex thickening in the pathophysiological sequence of AMD. Further longitudinal studies are needed, in particular to determine the value of RPE-BM thickening and PSL thinning measured using SD-OCT for the clinical follow-up of AMD patients.

Introduction

Age-related macular degeneration (AMD) is a complex multi-factorial disease and the leading cause of vision loss among older adults in high income countries.[1,2] Global pooled data of people between 45 and 85 years estimate the worldwide prevalence of AMD at 8.7%.[3]

AMD is classified into early, intermediate and advanced stages based on the severity of fundus lesions.[4] Early AMD may be asymptomatic and is characterized by medium-sized drusen (63-125 µm), which are clinically visible deposits of abnormal, incompletely degraded material beneath the retinal pigment epithelium (RPE). Further progression to intermediate AMD is marked by larger drusen (>125 µm) and pigmentary abnormalities of the macula. Advanced AMD includes atrophic AMD (geographic atrophy, GA) and neovascular AMD (choroidal neovascularization, CNV), both resulting in substantial visual decline in most patients.

Over the last decades, the understanding of AMD has greatly increased. Large epidemiological studies have identified risk factors such as cigarette smoking, nutritional factors, cardiovascular diseases, and genetic markers.[1,5] In 2016, a large genome-wide association study (GWAS) identified 52 genetic variants at 34 loci that are associated significantly with AMD. These 52 variants were used to compute a weighted polygenic risk score (PRS), which was estimated to account for more than half of the genomic heritability in the European-ancestry subjects.[6] The genes at these 34 loci are primarily involved in three biological pathways: the complement system, lipid metabolism, and extracellular matrix (ECM) remodeling.

Furthermore, multimodal imaging modalities such as optical coherence tomography (OCT) and fundus autofluorescence have made it possible to characterize in great detail the morphological changes in the course of AMD.[7] OCT changes in overall macular layer thickness and reflectivity are thus widely used for diagnosis and monitoring of AMD and other retinal and neurodegenerative diseases.[8–10] However, only in recent years automated OCT layer segmentation has made it possible to study in depth the changes in distinct macular layers in retinal disease.[11–13]

In normal aging, an overall thinning of the retina is observed, in particular due to loss of neurons.[14] Further, the aging RPE undergoes structural changes, including loss of melanin granules, increase in the number of residual bodies and accumulation of the age pigment lipofuscin.[15] It is thought that these changes lead to reduced antioxidant capacity of the RPE and progressive accumulation of basal laminar deposits (BLamDs) and formation of drusen.[16,17] BLamDs are histologically found between the RPE plasma membrane and its basal lamina and would thus be measured as part of the RPE layer in automated OCT layer segmentation.[18] Even though continuous enlarging BLamDs may indicate a strong risk for AMD progression and are accompanied by poor visual acuity and RPE dysmorphia, eyes with early BLamDs may show normal fundus appearance and visual acuity.[16]

Combined histopathological and functional studies have also evidenced that photoreceptor degeneration and loss, with a preferential vulnerability of rods, occur before disease progression to advanced AMD.[19–21]

Recent research showed that morphologic changes within the photoreceptors and RPE-Bruch's Membrane (BM) complex may be linked to AMD and its progression. There is also

some evidence of thinner photoreceptor segment layer (PSL) and thicker RPE-BM in individuals with high genetical susceptibility to AMD[22–25]. However, to date, there has been no longitudinal analysis of the different macular layer thicknesses in a population-based study in relation to AMD.

Thus, we analyzed the longitudinal associations of macular layer thicknesses, measured using spectral-domain OCT (SD-OCT) with incident intermediate and advanced AMD and AMD PRS in a population-based cohort of older adults.

Methods

Study cohort

The Alienor study is a prospective population-based cohort study. A total of 963 participants were recruited from 2006 through 2008 from the Bordeaux cohort of the Three City (3C) study. The 3C study was initiated in 1999 and recruited individuals aged 65 years or older from electoral registers. Both the Alienor study cohort and the 3C study cohort have been described in detail elsewhere.[5,26]

The Alienor study consists of biennial eye examinations at the Department of Ophthalmology of the University Hospital of Bordeaux between 2006 and 2024 (http://www.alienor-study.com/langue-english-1.html, accessed on 19 September 2024).

The Alienor study followed the tenets of the Declaration of Helsinki and was approved prospectively by the Ethical Committee of Bordeaux (Comité de Protection des Personnes Sud-Ouest et Outre-Mer III, code 2006/10) in May 2006. Informed consent of all participants of the Alienor study was obtained after explanation of the nature and possible consequences of the study.

Ophthalmic examination, retinal imaging and macular layer segmentation

The initial Alienor study protocol includes visual acuity, refraction, intraocular pressure and 45° high-resolution color fundus photographs (TRC NW6S; Topcon, Japan). Starting from the first follow-up visit (2009-2011), SD-OCT examinations of the macula and the optic nerve were included to the Alienor study protocol (Spectralis; Heidelberg Engineering, Germany). The same OCT device was used at all follow-up visits.

For the OCT acquisitions, a standardized imaging protocol was employed. All OCT assessments were performed by the same experienced technician. The Spectralis® OCT provides an automatic real-time function that adjusts for eye movement and increases image quality. For the macular cube acquisition, the following conditions were used: resolution mode, high speed; scan angle, 20°; number of B-scans, 19; pattern size, 20° × 15°; centered on the fovea and distance between B-scans, 236 µm. Single horizontal and vertical B-scan images (1536 A-scans) centered on the fovea were also performed.

The OCT-layer segmentation was performed using the inbuilt automated segmentation algorithm of the Heidelberg Eye Explorer (HEYEX 2) on the macular volume scan. The HEYEX segmentation algorithm delineates the following macular layers **(Figure 1)**: retinal nerve fiber layer (RNFL), ganglion cell layer (GCL), inner plexiform layer (IPL), inner nuclear layer (INL), outer plexiform layer (OPL), outer nuclear layer (ONL), and retinal pigment epithelium (RPE). With modern SD-OCT devices, the single band previously attributed to the RPE can now occasionally be seen as 2 distinctive hyperreflective bands separated by a hyporeflective zone, particularly when pathology is present. We thus used the term RPE-BM complex instead of RPE, consistent with recent literature.[27] Furthermore, the layers from RNFL to ONL are combined to inner retinal layers (IRL), the photoreceptors and the RPE-BM complex to outer retinal layers (ORL), and all layers to total retinal layers (TRL). An additional layer distinct to the above listed can be calculated by subtraction of the RPE-BM complex from the ORL. This layer represents the photoreceptor inner and outer segments including the interdigitation zone and we will refer to it as photoreceptor segment layer (PSL) in the following. For each layer, the device reports the average thickness (in µm) in nine sectors (center, superior inner, temporal

inner, inferior inner, nasal inner, superior outer, temporal outer, inferior outer and nasal outer) of the 6 mm diameter Early Treatment Diabetes Retinopathy Study (ETDRS) grid centered on the fovea. As a recent cross-sectional study showed associations between macular layer thicknesses and early AMD mainly in the central (1 mm in diameter) and inner circle (consisting of the superior inner, temporal inner, inferior inner and nasal inner sector, 1–3 mm) of the ETDRS grid,[24] we focused our analysis on those two circles. In addition, our macular cube is too small to assess the outer ETDRS circle. The mean thickness of the inner circle was determined by calculating the average of the four inner sectors: superior inner, temporal inner, inferior inner, nasal inner.

The accuracy and reproducibility of the inbuilt automated segmentation algorithm of the HEYEX has been previously reported.[28]

All available OCT data of the Alienor cohort were exported between January and April 2024. OCT images of participants with missing OCT data, retinal diseases and identified outliers as well as signal strength lower than 15 dB were ophthalmologically reviewed for segmentation quality. Acquisitions with artefacts and segmentation errors were excluded from the analysis.

Classification of AMD

For fundus photography, the AMD grading scheme followed the International Classification and Grading System by Bird et al., modified for drusen size, location and area according to the Multi-Ethnic Study of Atherosclerosis.[29,30] Grading was performed from color fundus photographs in duplicate by two trained graders and inconsistencies between the two graders were adjudicated by a retina specialist.[5] In addition, SD-OCT macular scans were interpreted for signs of advanced atrophic AMD and neovascular

AMD. Finally, classification of advanced AMD was performed by retina specialists, using all available information (ophthalmological history and treatments, color fundus photographs, SD-OCT scans).

To increase the comparability of this study with clinical routine data, in the present study, we used the Beckman AMD classification,[4] with intermediate AMD defined as presence of large drusen and/or pigmentary abnormalities on fundus photographs, in the absence of advanced AMD (atrophic and or neovascular).

Incidence of intermediate AMD was defined as the eye progressing from no or early AMD at baseline OCT examination (2009–2010) to intermediate AMD at any time-point during the study period (2009–2020). Incidence of advanced AMD was defined as the eye progressing from no, early AMD or intermediate at baseline OCT examination (2009–2010) to advanced AMD at any time-point during the study period (2009–2020). The date of occurrence of intermediate/advanced AMD was calculated as the midpoint of the interval between the last visit without intermediate /advanced AMD and the first visit with intermediate /advanced AMD.

Covariates

Polygenic risk score (PRS): Genotyping was performed by the French Centre National de Génotypage at 3C study baseline (1999–2001) using Illumina Human610-Quad BeadChips.[31] The present PRS is based on the weighted risk score published by Fritsche and colleagues and was described in detailed elsewhere.[6,32–34] The score corresponds to the sum of the corresponding betas multiplied by the number of minor alleles for each single nucleotide polymorphism (SNP). The betas used are calculated from the fully conditioned odds ratios of Fritsche et al. Due to the high number of missing data for the

three following SNPs: TRPM3 rs71507014, CNN2 rs67538026, and MMP9 rs142450006, these SNPs have been excluded from the risk score calculation. The present total PRS is thus based on 49 SNPs and was calculated for all participants who had available data for at least the five majors AMD-related genes (CFH rs10922109, CFH rs570618, C2 rs11603772, C3 rs2230199, and ARMS2 rs3750846).[32,34] The pathway-specific PRS were calculated for the three main biological pathways: C2, C3, C9, CFH, CFI and TMEM97 for the complement pathway, ADAMTS9, COL4A3, COL8A1, SYN3 and VEGFA for the ECM pathway and ABCA1, APOE, CETP, LIPC for the lipid pathway.[34] The PRS were used as quantitative variables after Z score standardization.

Sociodemographic data, lifestyle characteristics and medical variables were collected at 3C baseline.[26]

Medical variables including diabetes (fasting blood glucose ≥7 mmol/L and/or diabetes medication), hypertension (blood pressure >140/90 mm Hg and/or antihypertensive medication), and systemic lipid-lowering medications were also assessed at 3C baseline. Fasting plasma lipids were measured at the Biochemistry Laboratory of the University Hospital of Dijon, France using routine enzymatic techniques. Plasma esterified 3-hydroxy fatty acids (3-OH FAs) were quantified as a proxy of total plasma LPS burden using liquid chromatography tandem mass spectrometry (LC-tandem MS).[35] All plasma measurements were assessed using blood samples collected during the 3C baseline visit (1999–2001).

The Mediterranean diet score is based on MEDI-LITE score developed by Sofi et al.[36] This score is based on a 148-items validated food frequency questionnaire and reflects

the level of adherence to the Mediterranean diet, ranging from 0 (poor adherence) to 18 (highest adherence).

Statistical analyses

Cox proportional hazards model:

Associations of each macular layer thickness with incident intermediate / advanced AMD were estimated using Cox proportional hazards models. The individual eye was used as the unit of analysis. To take into account intra-individual correlation between eyes of one participant, the “cluster” term was included in the using Cox proportional hazards models in R (R Foundation for Statistical Computing, Vienna, Austria).

Time-dependent Cox proportional hazards model were used as an extension of the standard Cox model, allowing to include the repeated OCT measurements of macular layer thickness data.

Cox proportional hazards model was not performed for incident early AMD due to insufficient power, as 23.2 % (n = 223) of the cohort already had early AMD at baseline of this study.

All conditions for the application of the Cox model were verified. Linearity was checked using penalized splines with four degrees of freedom (pspline function in the Coxph function of R). The proportional hazard assumption was checked using Schoenfeld residuals.

Multivariate adjustments:

For the Cox proportional hazards model, we used two different sets of adjustments: Model 1 was adjusted for age at baseline and sex. Model 2 was further adjusted for the most

relevant potential confounders identified from the literature and with a directed acyclic graph (DAG). As some data on these variables were missing, we used multivariate imputation by chained equations (MICE) assuming that missing data were Missing At Random (MAR). Model 2 was thus adjusted after multivariate imputation.

Linear mixed model:

To study the evolution of each distinct macular layer thickness over the study period, we used linear mixed models (LMM), with the eye as the unit of analysis, as described previously.[37,38] One model was fitted per layer and the outcome variable of each model was the macular layer thickness by circle (central or inner). The longitudinal relationship of each macular layer thickness with the fixed effects age at baseline, sex and follow-up time was studied. Interactions of age at baseline with follow-up time and sex with follow-up time were not used, as the Akaike Information Criterion (AIC) and Bayesian Information Criterion (BIC) were favorable of the less complex models.

To study the longitudinal evolution of each macular layer according to the genetic risk of AMD, the fixed effects age, follow-up time and sex, as well as PRS and the interactions between PRS and follow-up time were included in LMMs.

Finally, three sensitivity analysis were performed using LMMs, the first also included AMD stage at baseline (no/early/intermediate/advanced) as fixed effect, the second excluded all participants with any AMD stage at baseline and the third excluded all participants with intermediate or advanced AMD stage at baseline.

All conditions for the application of the linear mixed model were verified. The linearity of quantitative variables was investigated using restricted cubic spline functions.

Correction for multiple testing

To address multiple testing, the Benjamini-Hochberg procedure was applied for false discovery rate (FDR) correction.[39] The Benjamini-Hochberg procedure adjusts p-values in a stepwise manner aiming to limit the proportion of false positives: After p-values are assigned ranks according to their ascending value, adjusted p-values were calculated using the following formula, where:

$$p\_adjusted_{(i)} = \min\left(1, \min_{k \geq i}\left(\frac{m}{k} \cdot p_{(k)}\right)\right)$$

- adjusted p(i) represents the adjusted p-value for the i-th ranked p-value,
- p(k) represents the k-th ranked p-value and
- m represents the total number of hypotheses being tested.

Statistical significance was determined using an FDR-corrected P value (P FDR) of less than 0.05.

R software version 4.3.3 (R Foundation for Statistical Computing, Vienna, Austria) was used for all statistical analyses.

Results

Characteristics of the studied sample

OCT examinations were included to the Alienor study protocol from 2009. Thus, the studied sample comprises all participants of the Alienor study receiving at least one OCT examinations between the first follow-up visit (2009-2010) and the last follow up visit in February 2024. A total of 3532 OCT scans of 721 subjects were exported. Of these 344 OCT scans of 94 subjects were excluded due to low quality. Further 408 OCT scans of 174 subjects were excluded due to errors of the automatic segmentation **(Figure S2)**. Thus, in total 2780 OCT examinations of 653 subjects were analyzed.

Among the 653 included participants, mean age at first OCT examination was 82.2 years (± 4.2) and 400 (61.3%) were female **(Table 1)**. Approximately two-thirds had never smoked and 15.8 % were obese (Body mass index, BMI > 30 kg/m2). Prevalent hypertension was reported in 473 (72.4 %) of the participants and prevalent diabetes mellitus in 46 (7.0 %). A total of 236 (36.1 %) participants received one OCT examination, 166 (25.4 %) received two, 109 (16.7 %) received three, 82 (12.6 %) received four and 60 (9.2 %) received at least five. For the 417 participants receiving more than one OCT examination, the average follow-up time was 4.8 years (range 0.3 to 14.1).

Measurements of Macular Layer Thicknesses

The thickness of eight separate macular layers and three compound layer complexes was measured in micrometers, including the RNFL, GCL, IPL, INL, OPL, ONL, PSL, RPE-BM complex, IRL complex and ORL complex and TRL complex. The mean macular layer

thicknesses of the 1 mm central and the 1 mm - 3 mm inner ETDRS circle of these layers and layer complexes at baseline OCT examination can be found in **Table S2**.

Macular layer thicknesses and the risk of incident intermediate and advanced AMD

We analyzed the associations of macular layer thicknesses with incident intermediate and advanced AMD. To take into account the data of all available OCT follow-up examinations, we used time-dependent proportional hazard Cox Models (**Table 3**).

Incident intermediate AMD: After adjustment for age and sex, we observed an association of incident intermediate AMD with thicker RPE-BM complex in the 1 mm central circle (Hazard ratio (HR) = 1.12 for 1 µm increase; 95% confidence interval (CI), [1.08; 1.18]; $P_{FDR} = 9.75 \times 10^{-4}$, **Table 3**). The association was similar after adjustment for AMD stage at baseline, high-density lipoprotein (HDL) cholesterol, low-density lipoprotein (LDL) cholesterol, triglycerides (TG), diet quality, body mass index (BMI), lipid-lowering medication, physical activity, 3-hydroxy fatty acids as a proxy of Lipopolysaccharide -type endotoxins, smoking and PRS (**Table 3**). No significant association was observed of incident intermediate AMD with any other macular layer, neither in the central circle, nor in the inner circle.

Incident advanced AMD: After adjustment for age and sex, the time-dependent Cox Model showed that thicker RPE-BM complex in the 1 mm central circle was associated with higher risk of advanced AMD (HR = 1.16 for 1 µm increase; 95% CI, [1.10; 1.22]; $P_{FDR} = 1.01 \times 10^{-7}$) (**Table 3**). The association was similar in the fully-adjusted model (**Table 3)**. Also, in the 1 – 3 mm inner circle, thicker RPE-BM complex was strongly associated with higher risk of advanced AMD in the age and sex adjusted model (HR = 1.42 for 1 µm

increase; 95% CI, [1.30; 1.56]; $P_{FDR} = 7.49 \times 10^{-13}$), as well as in the fully-adjusted model (HR = 1.28 for 1 µm increase; 95% CI, [1.16; 1.42]; $P_{FDR} = 1.61 \times 10^{-5}$, **Table 3, Figure 3**). This corresponds to a multiplication of the risk of advanced AMD by 3.43 for an RPE-BM complex of 15 µm and by 11.8 for an RPE-BM complex of 20 µm, in comparison with an RPE-BM complex of 10 µm, in the fully-adjusted model. **(Figure 3)**. We observed no statistically significant associations with other retinal layers.

Evolution of macular layers with age, sex and follow-up time

Using linear mixed model analysis, we analyzed the evolution of each macular layer in depth, first looking into the associations with age, sex and time (**Table S4, Figure S4**).

In the 1 mm central circle, the four innermost macular layers differed significantly at baseline according to sex, with female sex being significantly associated with thinner RNFL (Coefficient Beta (ß)= -1.13 µm for female sex; 95% CI, [−1.53; −0.73]; $P_{FDR} = 1.79 \times 10^{-7}$), GCL (ß = -1.62 µm for female sex; 95% CI, [−2.34; −0.90]; $P_{FDR} = 3.33 \times 10^{-5}$), IPL (ß = -1.75 µm for female sex; 95% CI, [−2.33; −1.17]; $P_{FDR} = 3.12 \times 10^{-8}$) and INL (ß = -3.90 µm for female sex; 95% CI, [−4.83; −2.97]; $P_{FDR} = 8.88 \times 10^{-15}$). Older age at baseline was significantly associated with thinner PSL at baseline (ß = -0.15 µm for 1 year of age increase; 95% CI, [−0.20; −0.09]; $P_{FDR} = 1.32 \times 10^{-6}$).

In the 1 – 3 mm inner circle, older age at baseline was associated with thinner GCL (ß = -0.31 µm for 1 year of age increase; 95% CI, [−0.43; −0.19]; $P_{FDR} = 1.47 \times 10^{-6}$) and thinner IPL (ß = -0.20 µm for 1 year of age increase; 95% CI, [−0.27; −0.13]; $P_{FDR} = 1.79 \times 10^{-7}$) at baseline. Again, the female sex was significantly associated with thinner INL (ß = -1.20 µm for female sex; 95% CI, −1.73; −0.68]; $P_{FDR} = 2.67 \times 10\text{-}5$) and also with

thinner ONL (ß = −3.37 µm for female sex; 95% CI, −4.70; −2.03]; $P_{FDR} = 3.23 \times 10^{-6}$) at baseline.

Macular layer thicknesses in the 1 – 3 mm inner circle all decreased significantly with follow-up time, except for RNFL which increased. In the 1 mm central circle, INL and RPE-BM complex increased with follow-up time, while ONL and PSL decreased.

AMD polygenic risk score (PRS) and macular layers

Using linear mixed model analysis, we then analyzed the association of each layer according to their genetic risk using the PRS for AMD, adjusting for age at baseline and sex (**Table S5**).

The AMD PRS was significantly associated with thinner PSL at baseline in the 1 mm central circle (ß= - 0.63 µm for 1 standard deviation (SD)-increase of the PRS, 95% CI, [-0.86; -0.40], $P_{FDR} = 2.42 \times 10^{-6}$, **Table S5, Figure 5**) and in the 1 – 3 mm inner circle (ß= -0.39, 95% CI [-0.52; -0.26], $P_{FDR} = 2.46 \times 10^{-7}$, **Table S5, Figure 5)**, but was not significantly associated with the evolution of PSL with follow-up time.

The AMD PRS was associated with a small but significant ONL thinning (ß= - 0.11 µm/ year for 1 SD-increase of the PRS, 95% CI, [-0.16; -0.06], $P_{FDR} = 3.08 \times 10^{-4}$, **Table S5**) and RPE-BM complex thickening (ß= 0.06 µm /year for 1 SD-increase of the PRS, 95% CI, [0.04; 0.07], $P_{FDR} = 1.61 \times 10^{-10}$, **Table S5**) in the 1 – 3 mm inner circle. As shown in **Figure 6**, ONL was not different at baseline in participants with high (standardized PRS = +1) or low (standardized PRS = -1) genetic susceptibility, but decreased more rapidly in those with high genetic susceptibility. Regarding the RPE-BM complex, again there was no significant difference at baseline between participants with high and low PRS, but RPE-

BM complex increased with time in those with high PRS, while it decreased in those with low PRS.

Of note, other layers were not associated with AMD PRS, either at baseline or during follow-up.

Three sensitivity analyses which showed similar results i) after inclusion of AMD stage (no/early/intermediate/advanced) at baseline as fixed effect, ii) after exclusion of all participants with any AMD at baseline and iii) after exclusion of all participants with intermediate and advanced AMD at baseline (**Table S6, S7 and S8**).

Pathway-specific polygenic risk scores (PRS) and macular layers

Using linear mixed model analysis, we analyzed the genetic risk profile in more detail by looking into the association of the pathway-specific PRS with the macular layers showing significant associations with the AMD PRS (**Table 9**).

We observed a significant association of the complement pathway with ONL thinning (ß= -0.16 µm/year, 95% CI [-0.21; -0.11], $P_{FDR} = 2.46 \times 10^{-7}$) in the 1 -3 mm inner circle, while ARMS2 was associated with ONL thickening in both the 1 mm central (ß= 0.12 µm/year, 95% CI [0.03; 0.21], $P_{FDR} = 0.04$) and the 1 -3 mm inner circle (ß= 0.09 µm/year, 95% CI [0.03; 0.15], $P_{FDR} = 0.02$, **Table 9**).

We also observed a significant association of the complement pathway with thinner baseline PSL in the 1 mm central circle (ß = -0.65 µm, 95 % CI [-0.93; -0.38], $P_{FDR} = 4.72 \times 10^{-5}$) and in the 1 – 3 mm inner circle (ß = - 0.40 µm, 95 % CI [-0.56; -0.25], $P_{FDR} = 6.66 \times 10^{-6}$). However, PSL decreased less rapidly with time in those with high complement

pathway PRS, both in the central (ß = 0.07 µm / year, 95 % CI [0.03; 0.11], P_{FDR} = 3.31 x 10^{-3}) and the inner circle (ß = 0.03 µm / year, 95 % CI [0.01; 0.05], P_{FDR} = 0.01, **Table 9)**. We did not observe significant associations of PSL with the other pathway-specific PRS.

Finally, we observed a significant association of the complement pathway (ß = 0.04 µm / year, 95 % CI [0.02; 0.06], P_{FDR} = 3.23 x 10^{-5}), the lipid pathway (ß = 0.03 µm / year, 95 % CI [0.02; 0.05], P_{FDR} = 3.74 x 10^{-4}) and ARMS2 (ß = 0.03 µm / year, 95 % CI [0.02; 0.05], P_{FDR} = 0.002) with RPE-BM complex thickening.

Discussion

This study evidenced a strong association between thicker foveal RPE-BM complex and both incident intermediate and advanced AMD. Longitudinal RPE-BM complex thickening was found to be strongly associated with total AMD PRS, and specifically with the complement, lipid metabolism and ARMS2 pathways PRS. Further, both the total AMD PRS and the complement-specific PRS were associated with thinner PSL at baseline and with longitudinal ONL thinning. Overall, our data contribute to and highlight the following results in the light of known pathophysiological mechanisms and recent literature.

First, RPE-BM complex thickening is a hallmark of AMD progression. In aging RPE cells, cumulative oxidative damage contributes to anatomical and physiological changes, including the accumulation of byproducts of the visual cycle leading to the accumulation of drusen (between the RPE basal lamina and Bruch's membrane).[40] Distinct of drusen, BLamDs, found between the RPE plasma membrane and its basal lamina, also represent early pathogenic changes in AMD.[16] Thus thickening of the RPE-BM complex measured using OCT possibly include drusen, BLamDs, accumulation of lipofuscin, increase in the density of residual bodies and diffuse thickening of Bruch's membrane.[14]

In 2019, a cross-sectional analysis of the German population-based AugUR Study also observed RPE-BM complex thickening and PSL thinning in early AMD.[24] Similarly, the cross-sectional Portuguese Coimbra study showed that RPE-BM complex thickening and PSL thinning is found in more severe early AMD.[25] Here, we show that RPE-BM complex is associated with future development of intermediate or advanced AMD, independently of potential confounders, including AMD stage at baseline.

Schmidt-Erfurth et al. used a machine learning–based predictive model assessing the risk of conversion to advanced AMD and described the reduction of neurosensory structures, including the PSL, as an important determinant in the progression to GA.[41] Further, they reported RPE-drusen complex thickening as a prominent predictor for the development of CNV. In the present study, however, we could not distinguish atrophic and neovascular AMD, due to the low number of incident advanced AMD cases.

A recent study by Zekavat et al., underlined the significance of early changes in the PSL, using the data of the UK Biobank with a broad AMD classification and including patients of an age span from 40 to 70 years.[22] They reported that PSL thinning and RPE-BM complex thickening were both significantly associated with increased AMD prevalence and incidence. Interestingly, they observed accelerated PSL thinning starting at around 45 years of age, 12 years before RPE-BM complex thickening, which highlights the potential pathophysiological sequence in morphological changes in the development of AMD.[22] This potential chronological sequence is in line with our finding of a highly significant association of RPE-BM complex thickening with incident intermediate and advanced AMD and could also explain the lack of finding PSL thinning, as this thinning might have occurred before the baseline OCT examination of our study cohort of participants aged 75 years or above at baseline.

Second, using repeated OCT measurements of the same individuals, we are the first to report the longitudinal evolution of each distinct macular layer according to age and gender in a cohort of people above the age of 75 at baseline. Using this data, we could show distinct sex-related differences, e.g. thinner inner macular layers in women which is in agreement with previous cross-sectional data.[28,42]

Third, our results showed that the total PRS based on 49 of the 52 genetic variants associated with AMD at a genome-wide significance level for AMD[6] was associated with thinner PSL at baseline. The total PRS was not associated with thicker RPE-BM complex at baseline, but with longitudinal RPE-BM complex thickening, which is again in line with the hypothesized pathophysiological chronological sequence of OCT-related changes by Zekavat et al.[22] Further, we also found an association between the total AMD PRS and longitudinal ONL thinning. This seems consistent with the cross-sectional data of Brandl et al. and Farinha et al. showing that ONL is decreased in participants with severe early AMD.[24,25]

Fourth, our results pinpoint specific mechanisms in PRS associated macular layer changes. The above used total PRS was grouped into four main biological pathways by an international consortium.[34] the complement system, lipid metabolism, ECM remodeling and ARMS2. Looking into those pathway specific PRS, the complement pathway was strongly associated with thinner PLS at baseline as well as longitudinal ONL thinning and RPE-BM complex thickening. Even though the genetic risk of AMD is considered to be linked to multiple genetic loci of small to modest effect, one of two major SNPs linked to advanced AMD is a variant in the complement factor H gene (CFH).[43–46] This variant affects the protein's ability to regulate inflammation, leading to increased susceptibility to chronic inflammation and damage in the retina. Associations with factor B and complement component C2 genes further emphasized the critical role of the complement system in the development of AMD.[47] Furthermore, systemic measurements of complement activation products like C3a, C3d, and C5a have consistently shown elevated levels in AMD.[48] However, using total macular thickness OCT data, a recent GWAS by

Gao et al. did not find an association between variants in the CFH gene within the outermost circle of the ETDRS grid.[49] By contrast, another study by Zouache et al. found that variants in the CFH gene were associated with perifoveal changes in macular thickness on OCT.[50] Finally, the study by Zekavat et al., reported the variants CFH:rs570618-T, CHF:10922109-C, CFH:rs187328863-T and ARMS2:rs3750846-C to be significantly associated with PSL thinning.[22]

Looking into the pathway specific PRS and longitudinal RPE-BM complex thickening reveals that multiple players are at game, of which the complement and lipid pathways seem to be strongest associated. However, in RPE-BM complex thickening, the second major AMD SNP, ARMS2, is also involved. Variants in this region are known to be associated with changes in mitochondrial function and increased inflammation, both contributing to retinal damage.[51–53]

Taken together, the current knowledge on morphologic and functional data indicates the importance of primarily RPE-BM complex thickening and photoreceptor degeneration/loss in the development of AMD. Further, similar to the normalized database of retinal nerve fiber measurements as used in glaucoma clinics, the use of RPE-BM complex measurements could be considered in AMD clinics. These measurements are readily available in the current version of the Heidelberg Spectralis. Longitudinal change of the RPE-BM complex might serve as an indicator of patients with high risk of conversion to advanced AMD.

The strengths of the study include a large and well-defined cohort, a detailed standardized ophthalmologic examination and long follow-up time. Although our prospective study

provides new insights into the genetic and morphologic correlation in AMD, limitations of this study have to be acknowledged: The OCT protocol performed systematically in the Alienor study employed 19 B-scans with an interscan distance of 236 µm, which implies that macular thickness values are based on a relatively limited number of scans. However, research on features of retinal diseases, in particular drusen volume and exudative retinal changes, has demonstrated that less dense scans (up to an interscan distance of 240 µm) do not significantly affect drusen volume measurements or impair the detection of exudative retinal changes.[8,54,55]

While the Heyex system's inbuilt segmentation algorithm is easily accessible, it may be less accurate than newer automated segmentation algorithms, especially when handling pathological alterations. To minimize the possibility of systematic misclassification of macular layer thicknesses, we manually reviewed all OCT scans with quality below 15dB, scans from patients with diagnosed retinal disease and any outliers (identified using linear regression). To ensure reproducibility, no manual corrections were performed, and all OCT scans with segmentations errors or disrupted retinal structure due to underlying disease were systematically excluded. Segmentation errors included missing retinal layers, overlapping or merging layers, incorrect retinal layer boundary detection, segmentation gaps, erroneous inclusion of pathological features in retinal layer. However, the measurement errors due to the acquisition protocol and the segmentation algorithm are most probably not differential and therefore would tend to attenuate the estimated associations. Future studies should strive to minimize such methodological limitations by using more numerous scans and more precise algorithms.

The genetic risk score used in this study is based on the foundational work by Fritsche et al. 2016, which identified key AMD risk SNPs.[6] However, due to the rapid advancements in genetic research, more recent studies have significantly expanded on this by providing higher SNP resolution, particularly through fine-mapping techniques. These advancements have enabled the identification of more specific, potentially causal variants at known risk loci, especially with the inclusion of multi-ethnic cohorts.[56,57] While these recent papers offer enhanced resolution, considering the European ethnicity of participants in the Alienor study, the comprehensive coverage of major AMD risk SNPs and the comparable discriminatory power, the use of the current PRS score based on Fritsche et al. 2016 remains justified.

Finally, we considered a wide range of potential cofounders but cannot exclude that some residual confounders or sources of misclassification could explain our observed association between RPE-BM complex thickening and incident intermediate and advanced AMD.

Conclusion

We found a strong association of thicker RPE-BM complex with incident intermediate and advanced AMD in a population-based cohort of elderly individuals. Thickening of the RPE-BM complex was also more pronounced in participants with high genetic susceptibility to AMD, as well as ONL thinning and thinner PSL at baseline. These results highlight the importance of RPE-BM complex thickening in the pathophysiological sequence of AMD. Further longitudinal studies are needed, in particular to determine the value of RPE-BM

505 complex thickening and PSL thinning measured using SD-OCT for the clinical follow-up
506 of AMD patients.

References

1. Guymer RH, Campbell TG. Age-related macular degeneration. *The Lancet*. 2023;401(10386):1459-1472. doi:10.1016/S0140-6736(22)02609-5

2. Fleckenstein M, Keenan TDL, Guymer RH, et al. Age-related macular degeneration. *Nat Rev Dis Primer*. 2021;7(1). doi:10.1038/s41572-021-00265-2

3. Wong WL, Su X, Li X, et al. Global prevalence of age-related macular degeneration and disease burden projection for 2020 and 2040: A systematic review and meta-analysis. *Lancet Glob Health*. 2014;2(2):e106-e116. doi:10.1016/S2214-109X(13)70145-1

4. Ferris FL, Wilkinson CP, Bird A, et al. Clinical classification of age-related macular degeneration. *Ophthalmology*. 2013;120(4):844-851. doi:10.1016/j.ophtha.2012.10.036

5. Delcourt C, Korobelnik JF, Barberger-Gateau P, et al. Nutrition and age-related eye diseases: The Alienor (Antioxydants, lipides essentiels, nutrition et maladies oculaires) study. *J Nutr Health Aging*. 2010;14(10):854-861. doi:10.1007/s12603-010-0131-9

6. Fritsche LG, Igl W, Bailey JNC, et al. A large genome-wide association study of age-related macular degeneration highlights contributions of rare and common variants. *Nat Genet*. 2016;48(2):134-143. doi:10.1038/ng.3448

7. Holz FG, Sadda SVR, Staurenghi G, et al. Imaging Protocols in Clinical Studies in Advanced Age-Related Macular Degeneration: Recommendations from Classification of Atrophy Consensus Meetings. *Ophthalmology*. 2017;124(4):464-478. doi:10.1016/j.ophtha.2016.12.002

8. Fang PP, Domdei N, Herrmann P, et al. Minimal optical coherence tomography B-scan density for reliable detection of intra- and subretinal fluid in macular diseases. *Retina*. 2019;39(1):150-156. doi:10.1097/IAE.0000000000001918

9. Grover S, Murthy RK, Brar VS, Chalam KV. Normative Data for Macular Thickness by High-Definition Spectral-Domain Optical Coherence Tomography (Spectralis). *Am J Ophthalmol*. 2009;148(2):266-271. doi:10.1016/j.ajo.2009.03.006

10. Hopf S, Tüscher O, Schuster AK. Retinal OCT biomarkers and neurodegenerative diseases of the central nervous system beyond Alzheimer's disease. *Ophthalmol*. 2024;121(2):93-104. doi:10.1007/s00347-023-01974-7

11. Keane PA, Grossi CM, Foster PJ, et al. Optical Coherence Tomography in the UK Biobank Study – Rapid Automated Analysis of Retinal Thickness for Large Population-Based Studies. Sørensen TL, ed. *PLOS ONE*. 2016;11(10):e0164095. doi:10.1371/journal.pone.0164095

12. Arnould L, Guillemin M, Seydou A, et al. Association between the retinal vascular network and retinal nerve fiber layer in the elderly: The Montrachet study. Grulkowski I, ed. *PLOS ONE*. 2020;15(10):e0241055. doi:10.1371/journal.pone.0241055

13. Emamverdi M, Vatanatham C, Fasih-Ahmad S, et al. Probing Deposit-Driven Age-Related Macular Degeneration Via Thicknesses of Outer Retinal Bands and Choroid: ALSTAR2 Baseline. *Invest Ophthalmol Vis Sci*. 2024;65(5):17. doi:10.1167/iovs.65.5.17

14. Bonilha V. Age and disease-related structural changes in the retinal pigment epithelium. *Clin Ophthalmol*. Published online June 2008:413. doi:10.2147/OPTH.S2151

15. Krohne TU, Stratmann NK, Kopitz J, Holz FG. Effects of lipid peroxidation products on lipofuscinogenesis and autophagy in human retinal pigment epithelial cells. *Exp Eye Res*. 2010;90(3):465-471. doi:10.1016/j.exer.2009.12.011

16. Sarks S, Cherepanoff S, Killingsworth M, Sarks J. Relationship of Basal Laminar Deposit and Membranous Debris to the Clinical Presentation of Early Age-Related Macular Degeneration. *Investig Opthalmology Vis Sci*. 2007;48(3):968. doi:10.1167/iovs.06-0443

17. Boulton M, Dayhaw-Barker P. The role of the retinal pigment epithelium: Topographical variation and ageing changes. *Eye*. 2001;15(3):384-389. doi:10.1038/eye.2001.141

18. Sura AA, Chen L, Messinger JD, et al. Measuring the Contributions of Basal Laminar Deposit and Bruch's Membrane in Age-Related Macular Degeneration. *Investig Opthalmology Vis Sci*. 2020;61(13):19. doi:10.1167/iovs.61.13.19

19. Curcio CA, Medeiros NE, Millican CL. Photoreceptor loss in age-related macular degeneration. *Invest Ophthalmol Vis Sci*. 1996;37(7):1236-1249.

20. Curcio CA. Photoreceptor topography in ageing and age-related maculopathy. *Eye*. 2001;15(3):376-383. doi:10.1038/eye.2001.140

21. Owsley C, Jackson GR, Cideciyan AV, et al. Psychophysical Evidence for Rod Vulnerability in Age-Related Macular Degeneration. 2000;41(1).

22. Zekavat SM, Sekimitsu S, Ye Y, et al. Photoreceptor Layer Thinning Is an Early Biomarker for Age-Related Macular Degeneration: Epidemiologic and Genetic Evidence from UK Biobank OCT Data. *Ophthalmology*. 2022;129(6):694-707. doi:10.1016/j.ophtha.2022.02.001

23. Ferrara D, Silver RE, Louzada RN, Novais EA, Collins GK, Seddon JM. Optical Coherence Tomography Features Preceding the Onset of Advanced Age-Related Macular Degeneration. *Investig Opthalmology Vis Sci*. 2017;58(9):3519. doi:10.1167/iovs.17-21696

24. Brandl C, Brücklmayer C, Günther F, et al. Retinal layer thicknesses in early age-related macular degeneration: Results from the German AugUR study. *Invest Ophthalmol Vis Sci*. 2019;60(5):1581-1594. doi:10.1167/iovs.18-25332

25. Farinha C, Silva AL, Coimbra R, et al. Retinal layer thicknesses and neurodegeneration in early age-related macular degeneration: insights from the Coimbra Eye Study. *Graefes Arch Clin Exp Ophthalmol*. 2021;259(9):2545-2557. doi:10.1007/s00417-021-05140-0

26. Alpérovitch A, Amouyel P, Dartigues JF, et al. Vascular Factors and Risk of Dementia: Design of the Three-City Study and Baseline Characteristics of the Study Population. *Neuroepidemiology*. 2003;22(6):316-325. doi:10.1159/000072920

27. Staurenghi G, Sadda S, Chakravarthy U, Spaide RF. Proposed lexicon for anatomic landmarks in normal posterior segment spectral-domain optical coherence tomography: The IN•OCT consensus. *Ophthalmology*. 2014;121(8):1572-1578. doi:10.1016/j.ophtha.2014.02.023

28. Mauschitz MM, Holz FG, Finger RP, Breteler MMB. Determinants of Macular Layers and Optic Disc Characteristics on SD-OCT: The Rhineland Study. *Transl Vis Sci Technol*. 2019;8(3):34. doi:10.1167/tvst.8.3.34

29. Bird AC, Bressler NM, Bressler SB, et al. An international classification and grading system for age-related maculopathy and age-related macular degeneration. *Surv Ophthalmol*. 1995;39(5):367-374. doi:10.1016/S0039-6257(05)80092-X

30. Klein R, Klein BEKK, Knudtson MD, et al. Prevalence of age-related macular degeneration in 4 racial/ethnic groups in the multi-ethnic study of atherosclerosis. *Ophthalmology*. 2006;113(3):373-380. doi:10.1016/j.ophtha.2005.12.013

31. Lambert JC, Heath S, Even G, et al. Genome-wide association study identifies variants at CLU and CR1 associated with Alzheimer's disease. *Nat Genet*. 2009;41(10):1094-1099. doi:10.1038/ng.439

32. Merle BMJ, Cougnard-Grégoire A, Korobelnik JF, et al. Plasma Lutein, a Nutritional Biomarker for Development of Advanced Age-Related Macular Degeneration: The Alienor Study. *Nutrients*. 2021;13(6):2047. doi:10.3390/nu13062047

33. De Breuk A, Acar IE, Kersten E, et al. Development of a Genotype Assay for Age-Related Macular Degeneration. *Ophthalmology*. 2021;128(11):1604-1617. doi:10.1016/j.ophtha.2020.07.037

34. Colijn JM, Meester-Smoor M, Verzijden T, et al. Genetic Risk, Lifestyle, and Age-Related Macular Degeneration in Europe. *Ophthalmology*. 2021;128(7):1039-1049. doi:10.1016/j.ophtha.2020.11.024

35. Pais de Barros JP, Gautier T, Sali W, et al. Quantitative lipopolysaccharide analysis using HPLC/MS/MS and its combination with the limulus amebocyte lysate assay. *J Lipid Res*. 2015;56(7):1363-1369. doi:10.1194/jlr.D059725

36. Sofi F, Dinu M, Pagliai G, Marcucci R, Casini A. Validation of a literature-based adherence score to Mediterranean diet: the MEDI-LITE score. *Int J Food Sci Nutr*. 2017;68(6):757-762. doi:10.1080/09637486.2017.1287884

37. Gayraud L, Mortamais M, Schweitzer C, et al. Association of long-term exposure to ambient air pollution with retinal neurodegeneration: the prospective Alienor study. *Environ Res*. 2023;232(May):116364. doi:10.1016/j.envres.2023.116364

38. Larsen PP, Feart C, Pais De Barros JP, et al. Association of lipopolysaccharide-type endotoxins with retinal neurodegeneration: the Alienor study. *Ophthalmol Sci*. Published online August 2024:100610. doi:10.1016/j.xops.2024.100610

39. Benjamini Y, Hochberg Y. Controlling the False Discovery Rate: A Practical and Powerful Approach to Multiple Testing. *J R Stat Soc Ser B Stat Methodol*. 1995;57(1):289-300. doi:10.1111/j.2517-6161.1995.tb02031.x

40. Johnson LV, Leitner WP, Staples MK, Anderson DH. Complement Activation and Inflammatory Processes in Drusen Formation and Age Related Macular Degeneration. *Exp Eye Res*. 2001;73(6):887-896. doi:10.1006/exer.2001.1094

41. Schmidt-Erfurth U, Waldstein SM, Klimscha S, et al. Prediction of Individual Disease Conversion in Early AMD Using Artificial Intelligence. *Investig Opthalmology Vis Sci*. 2018;59(8):3199. doi:10.1167/iovs.18-24106

42. Koh VT, Tham YC, Cheung CY, et al. Determinants of Ganglion Cell–Inner Plexiform Layer Thickness Measured by High-Definition Optical Coherence Tomography. *Investig Opthalmology Vis Sci*. 2012;53(9):5853. doi:10.1167/iovs.12-10414

43. Edwards AO, Ritter R, Abel KJ, Manning A, Panhuysen C, Farrer LA. Complement Factor H Polymorphism and Age-Related Macular Degeneration. *Science*. 2005;308(5720):421-424. doi:10.1126/science.1110189

44. Klein RJ, Zeiss C, Chew EY, et al. Complement Factor H Polymorphism in Age-Related Macular Degeneration. *Science*. 2005;308(5720):385-389. doi:10.1126/science.1109557

45. Haines JL, Hauser MA, Schmidt S, et al. Complement factor H variant increases the risk of age-related macular degeneration. *Science*. 2005;308(5720):419-421. doi:10.1126/science.1110359

46. Hageman GS, Anderson DH, Johnson LV, et al. A common haplotype in the complement regulatory gene factor H (HF1/CFH) predisposes individuals to age-related macular degeneration. *Proc Natl Acad Sci*. 2005;102(20):7227-7232. doi:10.1073/pnas.0501536102

47. Gold B, Merriam JE, Zernant J, et al. Variation in factor B (BF) and complement component 2 (C2) genes is associated with age-related macular degeneration. *Nat Genet*. 2006;38(4):458-462. doi:10.1038/ng1750

48. Kersten E, Paun CC, Schellevis RL, et al. Systemic and ocular fluid compounds as potential biomarkers in age-related macular degeneration. *Surv Ophthalmol*. 2018;63(1):9-39. doi:10.1016/j.survophthal.2017.05.003

49. Gao XR, Huang H, Kim H. Genome-wide association analyses identify 139 loci associated with macular thickness in the UK Biobank cohort. *Hum Mol Genet*. 2019;28(7):1162-1172. doi:10.1093/hmg/ddy422

50. Zouache MA, Bennion A, Hageman JL, Pappas C, Richards BT, Hageman GS. Macular retinal thickness differs markedly in age-related macular degeneration driven by risk polymorphisms on chromosomes 1 and 10. *Sci Rep*. 2020;10(1):21093. doi:10.1038/s41598-020-78059-x

51. Rivera A, Fisher SA, Fritsche LG, et al. Hypothetical LOC387715 is a second major susceptibility gene for age-related macular degeneration, contributing independently of complement factor H to disease risk. *Hum Mol Genet*. 2005;14(21):3227-3236. doi:10.1093/hmg/ddi353

52. Delcourt C, Delyfer MN, Rougier MB, et al. ARMS2 A69S Polymorphism and the Risk for Age-Related Maculopathy: The ALIENOR Study. *Arch Ophthalmol*. 2012;130(8):1077. doi:10.1001/archophthalmol.2012.420

53. Jakobsdottir J, Conley YP, Weeks DE, Mah TS, Ferrell RE, Gorin MB. Susceptibility Genes for Age-Related Maculopathy on Chromosome 10q26. *Am J Hum Genet*. 2005;77(3):389-407. doi:10.1086/444437

54. Garzone D, Terheyden JH, Morelle O, et al. Comparability of automated drusen volume measurements in age-related macular degeneration: a MACUSTAR study report. *Sci Rep*. 2022;12(1):1-10. doi:10.1038/s41598-022-26223-w

55. Thiele S, Nadal J, Fleckenstein M, et al. Longitudinal Analysis of Drusen Volume in Intermediate Age-Related Macular Degeneration Using Two Spectral-Domain Optical Coherence Tomography Scan Patterns. *Ophthalmologica*. 2018;239(2-3):110-120. doi:10.1159/000485260

56. He W, Han X, Ong JS, et al. Genome-Wide Meta-analysis Identifies Risk Loci and Improves Disease Prediction of Age-Related Macular Degeneration. *Ophthalmology*. 2024;131(1):16-29. doi:10.1016/j.ophtha.2023.08.023

57. Han X, Gharahkhani P, Mitchell P, Liew G, Hewitt AW, MacGregor S. Genome-wide meta-analysis identifies novel loci associated with age-related macular degeneration. *J Hum Genet*. 2020;65(8):657-665. doi:10.1038/s10038-020-0750-x

Figure Legends

Figure 1. Example of an auto- segmented spectral domain-OCT scan using the inbuilt automated segmentation of the Heidelberg Eye Explorer.
RNFL: retinal nerve fiber layer, GCL: ganglion cell layer, IPL: inner plexiform layer, INL: inner nuclear layer, OPL: outer plexiform layer, ONL: outer nuclear layer, PSL: photoreceptor segment layer, RPE-BM: retinal pigment epithelium- Bruch's Membrane complex.

Figure 3. Association between Retinal Pigment Epithelium (RPE) - Bruch's Membrane (BM) complex thickness within the 1 – 3 mm inner circle of the ETDRS grid and incident advanced AMD by eye, using time-dependent proportional hazards Cox Model, along with exemplary OCT photos of participants with an RPE - BM complex thickness of 10 µm, 15 µm and 20 µm at baseline. The model was adjusted for age, sex, high-density (HDL) cholesterol, low-density lipoprotein (LDL) cholesterol, triglycerides (TG), diet quality, body mass index (BMI), lipid-lowering medication, physical activity, 3-hydroxy fatty acids as a proxy of Lipopolysaccharide - type endotoxins, smoking status, polygenic risk score and AMD stage at baseline. AMD stage at baseline was categorized in 3 categories (no/early/intermediate). The hazard function is represented using p-spline with 4 degrees of freedom. Exemplary OCT images of participants with an RPE-BM complex thickness of 10 µm, 15 µm and 20 µm are shown. Data from the Alienor Study, 2009–2020.
HR: hazard ratio.

Figure 5. The evolution of photoreceptor segment layer (PSL) thinning over the follow-up time for both the 1 mm central and the 1 – 3 mm inner circle of the Early Treatment Diabetic Retinopathy Study (ETDRS) grid as predicted by linear mixed models (adjusted for age, sex and follow-up time) shown for the longitudinal relationship with standardized total (PRS) for AMD. The PRS was standardized using the formula $Z = (x-\mu)/\sigma$, where Z is the standard score, µ the mean and σ the standard deviation, respectively. Data from the Alienor Study, 2009–2024.

Figure 6. The evolution of the outer nuclear layer (ONL) and the retinal pigment epithelium (RPE) - Bruch's Membrane (BM) complex in the 1 – 3 mm inner circle of the Early Treatment Diabetic Retinopathy Study (ETDRS) grid over the follow-up time as predicted by linear mixed models (adjusted for age, sex and follow-up time) shown for the longitudinal relationship with standardized total polygenic risk score (PRS) for AMD. The PRS was standardized using the formula $Z = (x-\mu)/\sigma$, where Z is the standard score, µ the mean and σ the standard deviation, respectively. Data from the Alienor Study, 2009–2024.

Table 1. Baseline Characteristics of the Study Population (n = 653), Data from the Alienor Study.

Characteristics	Mean ± SD or n (%)
Age (years)	82.2 ± 4.2
Sex	
Male	253 (38.7 %)
Female	400 (61.3 %)
Smoking (pack-years)	
Never smoked	424 (64.9 %)
< 20	122 (18.7 %)
≥ 20	107 (16.4 %)
Body mass index (BMI)	
[0,18.5)	3 (0.5 %)
[18.5,25)	260 (39.8 %)
[25,30)	287 (44.0 %)
[30,59]	103 (15.8 %)
Plasma lipids (mmol/L)	
LDL cholesterol	3.6 ± 0.8
HDL cholesterol	1.6 ± 0.4
Triglycerides	1.2 ± 0.6
Diabetes	46 (7.0 %)
Hypertension	473 (72.4 %)
Cardiovascular Diseases	57 (8.7 %)
Mediterranean diet score	10.6 ± 2.0

LDL: low-density lipoprotein, HDL: high-density lipoprotein;
SD: standard deviation.

Table 3. Associations between the macular layer thicknesses and incidence of intermediate and advanced AMD. Alienor study, 2009–2020.

		Intermediate AMD (n = 103)				Advanced AMD (n = 39)			
		Central circle of the ETDRS grid		Inner circle of the ETDRS grid		Central circle of the ETDRS grid		Inner circle of the ETDRS grid	
		HR (95% CI)	P_{FDR}	HR (95% CI)	P_{FDR}	HR (95% CI)	P_{FDR}	HR (95% CI)	P_{FDR}
RNFL	Model 1	1.03 [0.97; 1.10]	0.62	1.00 [0.95; 1.05]	0.99	1.09 [0.97; 1.21]	0.53	1.06 [0.98; 1.15]	0.53
	Model 2	1.04 [0.97; 1.11]	0.60	1.00 [0.95; 1.06]	0.99	1.05 [0.93; 1.19]	0.69	1.04 [0.96; 1.13]	0.60
GCL	Model 1	1.01 [0.98; 1.04]	0.83	1.02 [0.99; 1.06]	0.53	1.03 [0.97; 1.09]	0.60	1.01 [0.96; 1.06]	0.83
	Model 2	1.02 [0.98; 1.05]	0.67	1.02 [0.99; 1.05]	0.54	1.02 [0.95; 1.08]	0.83	1.02 [0.97; 1.07]	0.73
IPL	Model 1	1.01 [0.96; 1.06]	0.92	1.03 [0.98; 1.08]	0.58	1.04 [0.96; 1.12]	0.60	1.00 [0.93; 1.08]	0.99
	Model 2	1.01 [0.96; 1.07]	0.83	1.03 [0.98; 1.08]	0.60	1.02 [0.95; 1.11]	0.75	1.02 [0.95; 1.10]	0.79
INL	Model 1	1.01 [0.98; 1.03]	0.74	0.99 [0.94; 1.04]	0.89	1.04 [1.01; 1.08]	0.13	1.03 [0.95; 1.12]	0.73
	Model 2	1.01 [0.98; 1.04]	0.60	0.98 [0.93; 1.03]	0.69	1.02 [0.98; 1.07]	0.60	1.01 [0.92; 1.11]	0.95
OPL	Model 1	1.00 [0.97; 1.03]	0.99	0.97 [0.93; 1.01]	0.55	0.99 [0.94; 1.06]	0.95	1.00 [0.93; 1.08]	0.99
	Model 2	1.00 [0.98; 1.03]	0.94	0.97 [0.93; 1.02]	0.55	1.00 [0.94; 1.06]	0.99	0.99 [0.92; 1.06]	0.90
ONL	Model 1	1.01 [1.00; 1.03]	0.54	1.01 [0.99; 1.04]	0.60	0.98 [0.95; 1.01]	0.60	0.95 [0.92; 0.99]	0.06
	Model 2	1.01 [0.99; 1.03]	0.60	1.01 [0.99; 1.03]	0.60	0.98 [0.95; 1.01]	0.53	0.96 [0.93; 0.99]	0.06
PSL	Model 1	0.97 [0.93; 1.03]	0.60	0.99 [0.90; 1.09]	0.94	0.93 [0.85; 1.03]	0.53	1.17 [1.04; 1.31]	0.07
	Model 2	0.97 [0.92; 1.03]	0.62	0.99 [0.89; 1.10]	0.95	0.96 [0.89; 1.04]	0.60	1.20 [1.02; 1.40]	0.14
RPE-BM	Model 1	**1.12 [1.06; 1.18]**	**9.75×10^{-4}**	1.09 [0.97; 1.22]	0.53	**1.16 [1.10; 1.22]**	**1.01×10^{-7}**	**1.42 [1.30; 1.56]**	**7.49×10^{-13}**
	Model 2	**1.13 [1.06; 1.20]**	**8.08×10^{-4}**	1.09 [0.97; 1.23]	0.53	**1.09 [1.04; 1.14]**	**0.005**	**1.28 [1.16; 1.42]**	**1.61×10^{-5}**

*For the inner circle, the thickness was calculated as the average of the nasal/temporal/superior/inferior subfields.

[a]Model 1, HR was estimated using Cox proportional model adjusted for age at baseline and sex. HR for 1 µm increase of the respective layer. [b]Model 2, HR was estimated using Cox proportional model adjusted for age, sex, high-density lipoprotein (HDL) cholesterol, low-density lipoprotein (LDL) cholesterol, triglycerides (TG), diet quality, body mass index (BMI), lipid-lowering medication, physical activity, 3-hydroxy fatty acids as a proxy of Lipopolysaccharide -type endotoxins, smoking, polygenic risk score and AMD stage at baseline. For intermediate AMD, AMD stage at baseline was in 2 categories (no/early), for advanced AMD, it was in 3 categories (no/early/intermediate). HR for 1 µm increase of the respective layer. ETDRS: Early Treatment Diabetic Retinopathy Study, CI: Confidence interval, FDR: false discovery rate, HR, hazard ratio, RNFL: retinal nerve fiber layer, GCL: ganglion cell layer, IPL: inner plexiform layer, INL: inner nuclear layer, OPL: outer plexiform layer, ONL: outer nuclear layer, PSL: photoreceptor segment layer, RPE-BM: retinal pigment epithelium- Bruch's Membrane complex.

Table 9. Longitudinal change of ONL, PSL and RPE-BM complex according to pathway-specific polygenic risk scores for AMD, Alienor study, 2009–2024. (n = 2780 examinations of 653 participants)

		Central Circle of the ETDRS Grid		Inner Circle of the ETDRS Grid*	
		β [95% CI]	P_{FDR}	β [95% CI]	P_{FDR}
ONL	Complement Pathway PRS**	0.04 [-0.89; 0.97]	0.99	0.11 [-0.62; 0.83]	0.94
	Complement Pathway PRS * Time	-0.09 [-0.17; -0.01]	0.12	**-0.16 [-0.21; -0.11]**	**2.46×10^{-7}**
	Extracellular Matrix Pathway PRS***	0.22 [-0.70; 1.14]	0.88	0.11 [-0.61; 0.83]	0.94
	Extracellular Matrix Pathway PRS * Time	0.02 [-0.06; 0.10]	0.84	-0.03 [-0.08; 0.02]	0.53
	Lipid Pathway PRS****	-0.30 [-1.22; 0.62]	0.81	0.06 [-0.66; 0.78]	0.97
	Lipid Pathway PRS * Time	-0.02 [-0.10; 0.06]	0.88	-0.02 [-0.07; 0.03]	0.72
	ARMS2	-0.16 [-1.09; 0.78]	0.94	-0.16 [-0.88; 0.57]	0.91
	ARMS2 * Time	**0.12 [0.03; 0.21]**	**0.04**	**0.09 [0.03; 0.15]**	**0.02**
PSL	Complement Pathway PRS**	**-0.65 [-0.93; -0.38]**	**4.72×10^{-5}**	**-0.40 [-0.56; -0.25]**	**6.66×10^{-6}**
	Complement Pathway PRS * Time	**0.07 [0.03; 0.11]**	**3.31×10^{-3}**	**0.03 [0.01; 0.05]**	**0.01**
	Extracellular Matrix Pathway PRS***	-0.17 [-0.45; 0.11]	0.50	-0.04 [-0.19; 0.12]	0.88
	Extracellular Matrix Pathway PRS * Time	-0.02 [-0.06; 0.02]	0.53	-0.002 [-0.02; 0.02]	0.94
	Lipid Pathway PRS****	-0.18 [-0.46; 0.09]	0.45	-0.11 [-0.27; 0.04]	0.36
	Lipid Pathway PRS * Time	0.01 [-0.03; 0.05]	0.94	-0.01 [-0.03; 0.01]	0.69
	ARMS2	-0.22 [-0.50; 0.06]	0.34	-0.16 [-0.31; 0.00]	0.16
	ARMS2 * Time	-0.02 [-0.07; 0.02]	0.56	-0.02 [-0.04; 0.01]	0.39
RPE-BM	Complement Pathway PRS**	-0.10 [-0.35; 0.15]	0.69	-0.21 [-0.38; -0.05]	0.05
	Complement Pathway PRS * Time	0.05 [0.004; 0.09]	0.11	**0.04 [0.02; 0.06]**	**3.23×10^{-5}**
	Extracellular Matrix Pathway PRS***	0.002 [-0.24; 0.25]	0.99	-0.02 [-0.18; 0.14]	0.94
	Extracellular Matrix Pathway PRS * Time	-0.01 [-0.05; 0.03]	0.93	0.002 [-0.01; 0.02]	0.94
	Lipid Pathway PRS****	0.004 [-0.24; 0.25]	0.99	-0.09 [-0.25; 0.07]	0.56
	Lipid Pathway PRS * Time	-0.001 [-0.04; 0.04]	0.99	**0.03 [0.02; 0.05]**	**3.74×10^{-4}**
	ARMS2	0.18 [-0.06; 0.43]	0.34	0.15 [-0.02; 031]	0.23
	ARMS2 * Time	0.003 [-0.04; 0.05]	0.99	**0.03 [0.02; 0.05]**	**0.002**

Mixed linear models are adjusted for age, sex and follow-up time. β in µm for 1-SD increase in PRS and in µm / year for 1-SD increase in PRS for the interaction with follow-up time. ETDRS: Early Treatment Diabetes Retinopathy Study, CI: confidence interval, FDR: false discovery rate, SD: standard deviation, ONL: outer nuclear layer, PSL: photoreceptor segment layer, RPE-BM: retinal pigment epithelium- Bruch's Membrane complex, SD: standard deviation.

*For the inner circle, the thickness was calculated as the average of the nasal/temporal/superior/inferior subfields.

**The Complement Pathway is based on the following genes: C2, C3, C9, CFH, CFI, TMEM97.

***The Extracellular Matrix Pathway is based on the following genes: ADAMTS9, COL4A3, COL8A1, SYN3, VEGFA.

****The Lipid Pathway is based on the following genes: ABCA1, APOE, CETP, LIPC.

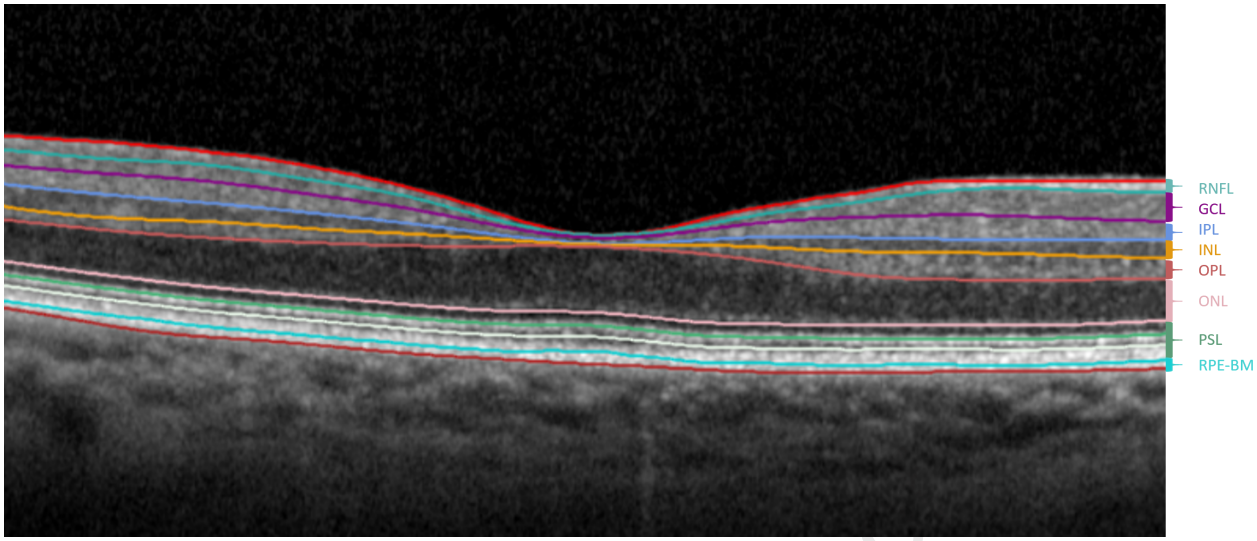

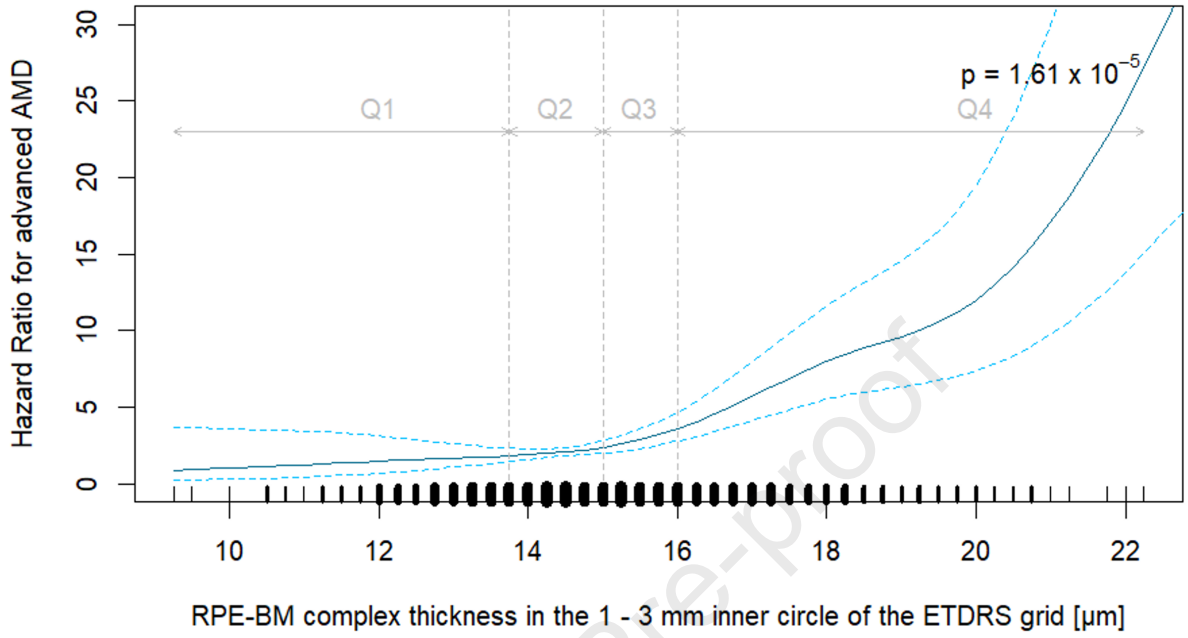

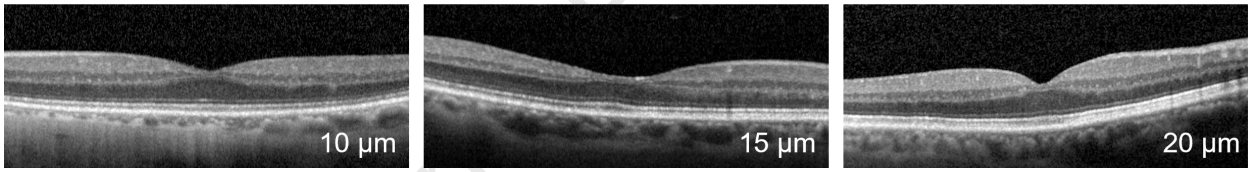

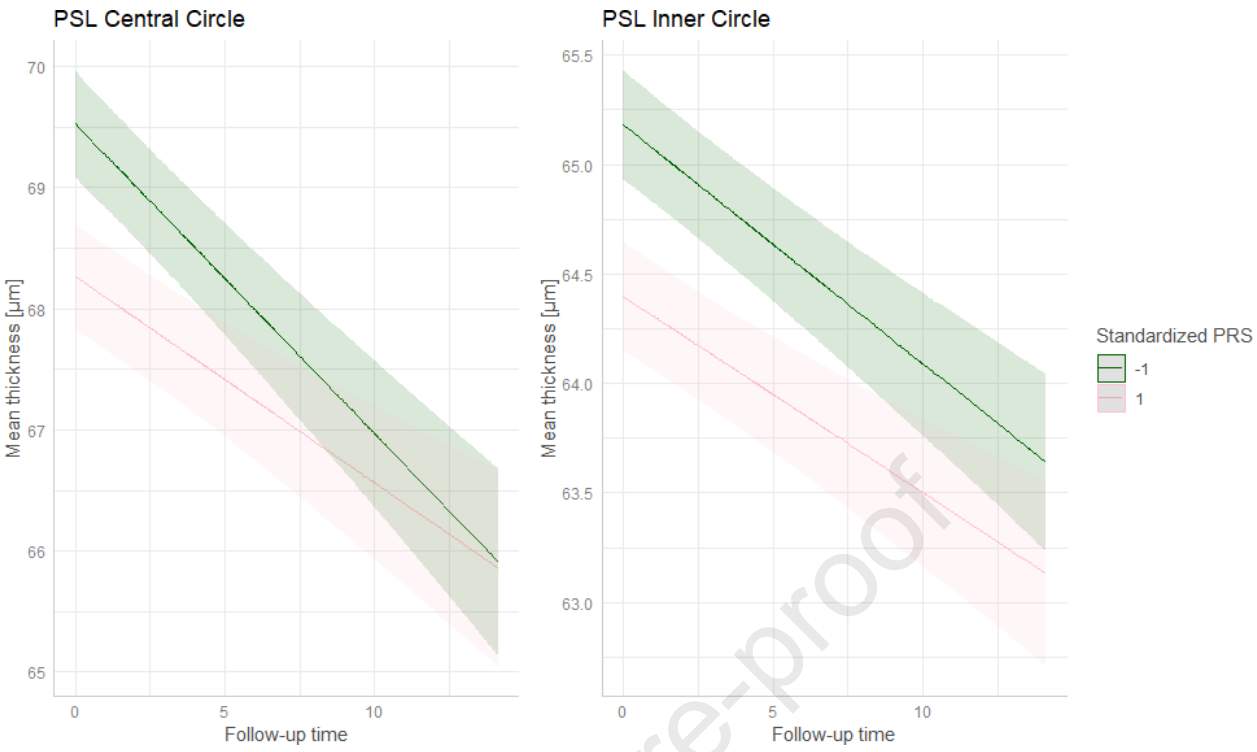

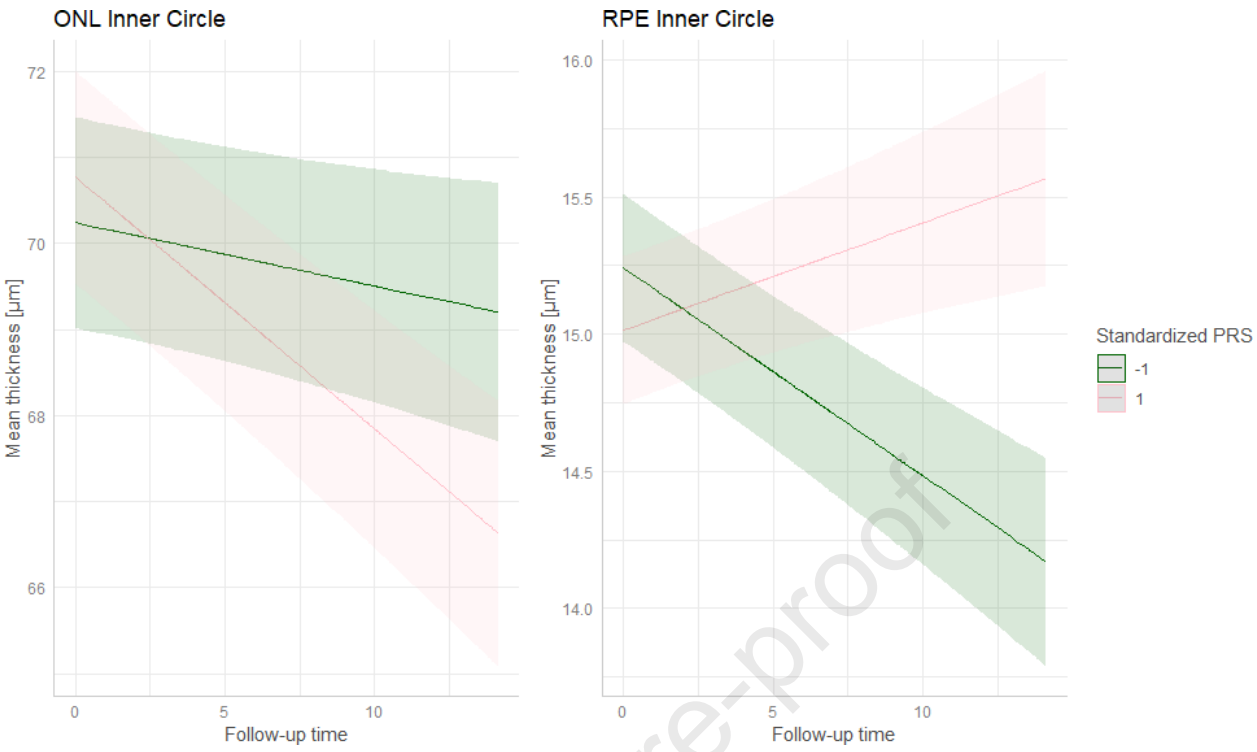

Précis

A strong association of RPE-BM complex thickening with both incident AMD and the genetic risk for AMD was evidenced, highlighting its pivotal role in the clinical course of AMD.